

Simultaneous Recognition of a Carboxylate-Containing Ligand and an Intramolecular Surrogate Ligand in the Crystal Structure of an Asymmetric Vancomycin Dimer

Patrick J. Loll,* Anthony E. Bevivino, Brian D. Korty, and Paul H. Axelsen*

Contribution from the Department of Pharmacology and the Johnson Foundation for Molecular Biophysics, University of Pennsylvania School of Medicine, 3620 Hamilton Walk, Philadelphia, Pennsylvania 19104-6084

Received October 14, 1996[⊗]

Abstract: Vancomycin is one of the most important and commonly used antibiotics in hospitals. Despite numerous investigations, however, it is not clear how vancomycin recognizes its site of action in the bacterial cell wall. The increasing incidence of bacterial resistance to vancomycin makes it imperative to understand these recognition determinants so that alternative agents may be developed. Herein we report the first crystal structure of vancomycin. The structure resolves a long-standing controversy about carboxylate recognition by vancomycin, suggests a possible cooperative mechanism linking ligand binding and dimerization, and demonstrates the operation of a novel intramolecular flap which occupies the binding site in the absence of ligand.

Introduction

Vancomycin is a natural product of *Nocardia orientalis* belonging to the class of drugs known as glycopeptide antibiotics. It is the only antibiotic in this class in common clinical use, and efforts to develop clinically superior or even useful alternatives have met with limited success. Vancomycin binds stereospecifically to the carboxy-terminal D-Ala-D-Ala sequences of peptidoglycan intermediates produced during bacterial cell wall biosynthesis, thereby inhibiting the action of bacterial enzymes that would otherwise use these termini to form new cross-links in peptidoglycan.^{1,2} A plasmid mediating resistance to vancomycin is beginning to appear with alarming frequency among bacteria that had long been uniformly susceptible.^{3,4} This plasmid makes possible the biosynthesis of peptidoglycan via carboxy-terminal D-alanyl-D-lactate (depsipeptide) intermediates, and can be exchanged among various gram positive bacterial species. There are no antimicrobial agents that are reliably effective against bacteria with this form of resistance, and new therapeutic agents that have an affinity for depsipeptide ligands are urgently needed.

The development of new glycopeptide antibiotics has been hindered by an incomplete understanding of ligand recognition by vancomycin and related compounds. A crystal structure of vancomycin has eluded investigators for over 30 years, most likely owing to the large size of the molecule and the difficulty of preparing suitable crystals. Partial success was reported by Sheldrick and colleagues,⁵ who determined the structure of a deaminated degradation product. This was later shown to differ from vancomycin in several critical features.^{6,7} More recently,

Sheldrick et al.⁸ reported a structure for the ureido derivative of a closely related compound, balhimycin.

The lack of a crystal structure of vancomycin, particularly of a ligand-bound form, has spurred numerous investigations using NMR.^{9–18} These investigations have been very successful at establishing accurate chemical structures and at demonstrating important structural features such as the asymmetric dimer. However, they have been unable to establish definitive and detailed structures for antibiotic:ligand complexes, leaving important conclusions to be inferred from molecular models and computer simulations.^{13,14,17,19} As a consequence, the hydrogen bond pattern and the role of at least two amino acid side chains remained unclear.

This paper describes the atomic resolution crystal structure of a vancomycin:acetate complex. It resolves a long-standing ambiguity about the binding mode of carboxylate-containing ligands, demonstrates the operation of a novel intramolecular flap which occupies the binding site in the absence of ligand, and suggests a possible cooperative mechanism linking ligand

(7) Williamson, M. P.; Williams, D. H. *J. Am. Chem. Soc.* **1981**, *103*, 6580–6585.

(8) Sheldrick, G. M.; Paulus, E.; Vertesy, L.; Hahn, F. *Acta Crystallogr.* **1995**, *B51*, 89–98.

(9) Brown, J. P.; Terenius, L.; Feeney, J.; Burgen, A. S. *Mol. Pharmacol.* **1975**, *11*, 126–132.

(10) Convert, O.; Bongini, A.; Feeney, J. *J. Chem. Soc. Perkin Trans.* **1980**, *1*, 1262–1270.

(11) Bongini, A.; Feeney, J.; Williamson, M. P.; Williams, D. H. *J. Chem. Soc. Perkin Trans.* **1981**, *2*, 201–206.

(12) Williams, D. H.; Williamson, M. P.; Butcher, D. W.; Hammond, S. J. *J. Am. Chem. Soc.* **1983**, *105*, 1332–1339.

(13) Prowse, W. G.; Kline, A. D.; Skelton, M. A.; Loncharich, R. J. *Biochemistry* **1995**, *34*, 9632–9644.

(14) Fesik, S. W.; O'Donnell, T. J.; Gampe, R. T. J.; Olegniczak, E. T. *J. Am. Chem. Soc.* **1986**, *108*, 3165–3170.

(15) Hawkes, G. E.; Molinari, H.; Singh, S.; Lian, L. Y. *J. Magn. Reson.* **1987**, *74*, 188–192.

(16) Barna, J. C. J.; Williams, D. H. *Annu. Rev. Microbiol.* **1984**, *38*, 339–357.

(17) Molinari, H.; Pastore, A.; Lian, L.; Hawkes, G. E.; Sales, K. *Biochemistry* **1990**, *29*, 2271–2277.

(18) Pierce, C. M.; Williams, D. H. *J. Chem. Soc. Perkin Trans.* **1995**, *2*, 153–157.

(19) Li, D.; Puga, F. J. I.; Frohner, P. M.; Axelsen, P. H. *J. Mol. Recog.* In press.

* Address correspondence to these authors.

[⊗] Abstract published in *Advance ACS Abstracts*, February 1, 1997.

(1) Marshall, F. J. *J. Med. Chem.* **1965**, *8*, 18–22.

(2) Nagarajan, R. *Glycopeptide Antibiotics*; Marcel Dekker, Inc.: New York, 1994.

(3) Arthur, M.; Courvalin, P. *Antimicrob. Agents Chemother.* **1993**, *37*, 1563–1571.

(4) Walsh, C. T. *Science* **1993**, *261*, 308–309.

(5) Sheldrick, G. M.; Jones, P. G.; Kennard, O.; Williams, D. H.; Smith, G. A. *Nature* **1978**, *271*, 223–225.

(6) Harris, C. M.; Kopecka, H.; Harris, T. M. *J. Am. Chem. Soc.* **1983**, *105*, 6915–6922.

Table 1. Crystal Data, Data Collection and Refinement Statistics

formula	C ₆₆ H ₇₅ Cl ₂ N ₉ O ₂₄ ·2HCl
formula wt	1,486
temperature	98 K
wavelength	0.85 Å
space group	<i>P</i> ₄ ₃ ₂ ₁ ₂
unit cell dimensions	
<i>a</i> = <i>b</i>	28.45(7) Å
<i>c</i>	65.8(2) Å
α = β = γ	90°
unit cell volume	53259 Å ³
<i>Z</i>	16
density	1.203 g/cm ³
max resolution for data collection	0.89 Å ($\theta = 28.5^\circ$)
no. of observations	228786
no. of independent reflcns	17828
<i>R</i> _{merge}	0.076
percentage of reflcns with <i>I</i> σ(<i>I</i>) > 4.0	
entire data set, 8–0.90 Å	85.8%
0.90–0.95 Å shell	69.3%
refinement terms	
no. of reflcns	17,645
no. of restraints	4274
no. of parameters	2553
final <i>R</i>	
<i>R</i> ₁	0.112
<i>wR</i> ₂	0.316
goodness of fit on <i>F</i> ²	1.13
highest and lowest peaks in difference Fourier	0.70/–0.39 electrons·Å ^{–3}

binding and dimerization. This information will facilitate the rational development of new therapeutic agents in this class.

Experimental Section

Materials. Pharmaceutical grade vancomycin hydrochloride (Vancomycin, Eli Lilly) was used without further purification. Other materials were of the highest purity available commercially.

Crystallization and Data Collection. Crystals were grown by the hanging drop vapor diffusion method. Five microliters of a 25 mg·mL^{–1} aqueous solution of vancomycin hydrochloride were mixed with an equal volume of 2.2 M NaCl, 0.1 M sodium acetate, pH 4.6 (reservoir buffer); the resulting drop was placed on a siliconized cover slip, inverted over a well containing 1 mL of reservoir buffer, and incubated at 20 °C. Bipyramidal crystals appeared within 1–3 weeks, with the largest dimension ≈0.6 mm. Crystal density was measured in a Ficoll gradient;²⁰ the measured value of 1.203 g/cm³ corresponds to a Matthews V_m number of 2.3 Å³/dalton,²¹ indicating that the asymmetric unit contained a vancomycin dimer.

Several days prior to data collection, crystals were transferred to a solution of 25% (v/v) glycerol in reservoir buffer. Immediately before data collection, crystals were mounted in a fiber loop and flash-cooled by plunging into liquid N₂. Crystals were maintained at –175 °C in a stream of N₂ gas during data collection.

Diffraction data were taken using a CCD area detector mounted on a 4-circle goniostat at beamline X8-C of the Argonne National Laboratory at the National Synchrotron Light Source²² with a crystal-to-detector distance of 140 mm. Intensities from individual scans taken from two different crystals were processed using the MADNES and PROCOR programs;^{23,24} these scans were combined into the final data set with the program XSCALE. Data collection statistics are given in Table 1.

Structure Solution and Refinement. Efforts to solve the vancomycin structure using heavy atom methods and molecular replacement met with no success. Ultimately, the problem was solved using direct methods, which proved challenging because of the large size of the vancomycin unit cell (the difficulty of direct phasing is dependent upon

the total number of atoms in the primitive cell; at 5.3×10^4 Å³, the volume of the vancomycin cell is considerably larger than that of many proteins, including rubredoxin at 1.9×10^4 Å³, tris(1,2-ethylenediyl)lysine at 2.6×10^4 Å³, and calmodulin at 3.9×10^4 Å³). This structure appears to rank among the largest determined by direct methods to date, and our success must be attributed to improved strategies for solving the phase problem²⁵ and to the availability of increasingly powerful computing technology.

The program SnB²⁶ was used for phase determination. *E* values were generated with the programs LEVY and EVAL²⁷ and input to the Shake-and-Bake phasing algorithm. Five thousand trial structures were generated in both *P*₄₃₂₁₂ and *P*₄₁₂₁₂. Each trial structure was subjected to 110 cycles of iterative structure factor calculation, phase refinement, and density modification. Phase refinement used a 90° parameter shift protocol, and density modification was carried out using automated peak-picking from the Fourier maps. From the 2×5000 trial structures examined, a single solution emerged in each of the two space groups. The refined value of the minimal function^{28,29} for both solutions was 0.48; the lowest minimal function value obtained for an incorrect solution was 0.53. The minimal function value for the correct solutions differed from the mean of the minimal function histograms by over 8 standard deviations.

Examination of the two solutions showed them to be approximate mirror images of each other; comparison with the known stereochemistry indicated that the correct space group was *P*₄₃₂₁₂. Solutions produced by SnB take the form of atomic positions inferred from the peaks in the final Fourier map. Inspection of the *P*₄₃₂₁₂ solution revealed three chemically sensible fragments comprising 104 atoms, including the 4 chlorine atoms. Two cycles of tangent expansion³⁰ using the program SHELXS-86³¹ yielded positions for 181 of the expected 202 non-hydrogen vancomycin atoms. We commenced refinement of this structure using SHELXL-93.³² Remaining atoms (including solvent water and chloride ions) were positioned by cycles of successive refinement and map calculation.

Refinement was carried out against *F*² using chemically reasonable restraints on the molecular geometry and atomic displacement parameters. The two vancomycin molecules in the asymmetric unit were restrained to have similar 1,2 and 1,3 distances; in addition, restraints were imposed to limit deviations from planarity and differences in along-bond components of anisotropic thermal parameters. Anisotropic thermal parameters for solvent waters were restrained to be approximately isotropic, and “anti-bumping” restraints were applied to discourage poorly ordered water molecules from violating minimum reasonable contact distances. A conjugate gradient protocol was used for most of the refinement, with blocked least-squares methods being used at the end of the refinement. Low-resolution reflections showed higher than normal *R*_{merge} values, most likely caused by overload problems encountered with very bright reflections and by localized noise introduced within the low-resolution area of the diffraction image by the detector’s image intensifier. For these reasons, reflections below 4 Å resolution were excluded from the final stages of the refinement. Hydrogen atom positions for the antibiotic were refined with a riding model; solvent hydrogen atoms were not included in the model. Three atom groups were each modeled as two conformers with occupancies summing to 1.0: The leucine amino acid side chain in molecule 1, the asparagine amino acid side chain in molecule 2, and the glucose moiety in molecule 2. Seven water molecules were also modeled as being distributed between two positions. The final model for the contents of the asymmetric unit comprises 2 vancomycin molecules, 1 acetate ligand, 4 chloride ions, and 48 water molecules. These atoms do not fill the entire asymmetric unit; calculations based on the difference

(25) Miller, R.; DeTitta, G. T.; Jones, R.; Langs, D. A.; Weeks, C. M.; Hauptman, H. A. *Science* **1993**, *259*, 1430–1433.

(26) Miller, R.; Gallo, S. M.; Khalak, H. G.; Weeks, C. M. *J. Appl. Crystallogr.* **1994**, *27*, 613–621.

(27) Blessing, R. H. *J. Appl. Crystallogr.* **1989**, *22*, 396–397.

(28) DeTitta, G. T.; Weeks, C. M.; Thuman, P.; Miller, R.; Hauptman, H. A. *Acta Crystallogr.* **1994**, *A50*, 203–210.

(29) Weeks, C. M.; DeTitta, G. T.; Hauptman, H. A.; Thuman, P.; Miller, R. *Acta Crystallogr.* **1994**, *A50*, 210–220.

(30) Karle, J. *Acta Crystallogr.* **1968**, *B24*, 182.

(31) Sheldrick, G. M. *Acta Crystallogr.* **1990**, *A46*, 467–473.

(32) Sheldrick, G. M. *J. Appl. Crystallogr.* In preparation.

(20) Westbrook, E. M. *Methods Enzymol.* **1985**, *114*, 187–196.

(21) Matthews, B. W. *Methods Enzymol.* **1985**, *114*, 176–187.

(22) Strauss, M. G.; Westbrook, E. M.; Naday, I.; Coleman, T. A.; Westbrook, M. L.; Travis, D. J.; Sweet, R. M.; Pflugrath, J. W.; Stanton, M. *Nucl. Instrum. Methods Phys. Res.* **1990**, *A297*, 275–295.

(23) Messerschmidt, A.; Pflugrath, J. W. *J. Appl. Crystallogr.* **1987**, *20*, 306–315.

(24) Kabsch, W. *J. Appl. Crystallogr.* **1988**, *21*, 916–924.

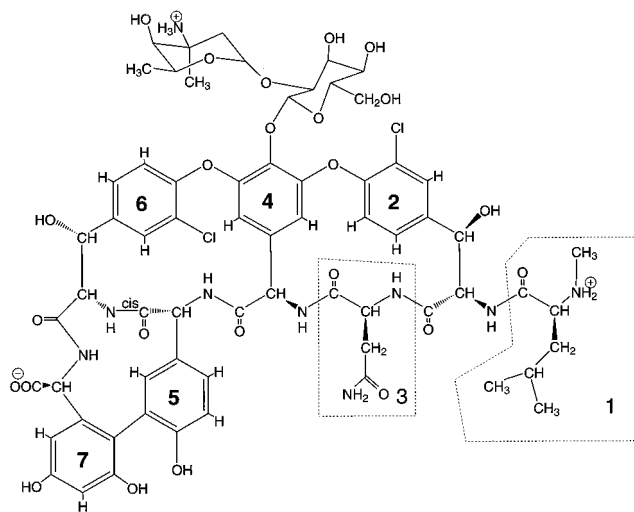


Figure 1. Chemical structure of the vancomycin monomer. Individual amino acid residues are numbered 1 through 7; the glucose and vancosamine sugars are labeled “G” and “V”, respectively.

between observed and calculated crystal densities show that roughly 25% of the volume of the unit cell is given over to channels filled with disordered solvent.

In the text below, the two independent molecules of vancomycin are designated V1 and V2 with the seven individual amino acid residues within each monomer designated V1:1, V1:2,...V1:7, and V2:1, V2:2,...V2:7 (Figure 1). The glucose and vancosamine residues will be indicated with “G” or “V” in place of a residue number. The acetate molecule is bound to V2, and the 4 chloride ions are designated Cl-1...Cl-4.

Structure Quality. The standard deviations of bond lengths and angles, estimated from the correlation matrices used in the blocked least-squares refinement,³³ range from 0.007 to 0.029 Å (mean = 0.010 Å) for bond lengths and from 0.4° to 1.8° (mean = 0.7°) for bond angles. Standard deviations obtained in this way are likely to be underestimated by a factor of 1.5–2.0;^{34,35} values that have been adjusted accordingly are in good agreement with an estimate of 0.03 Å for the root-mean-square coordinate error obtained by the method of Luzzati.³⁶ The bond lengths agree well with standard values,³⁷ and the thermal ellipsoids are reasonable in size and chemically sensible (Figure 2). The crystallographic residual is higher than might be expected; we attribute this to the relatively weak scattering of these crystals and to systematic errors introduced by localized noise in the image intensifier of the CCD detector. These latter errors are manifested as unusually high merging *R* values for strong moderate-to-low-resolution reflections which vary as functions of reflection position on the detector face, but not of resolution; the affected reflections then contribute to an unusually high crystallographic *R* in the low-resolution range (e.g., *R* = 0.10 for data between 1.6 and 2.0 Å, while *R* = 0.07 for data between 1.1 and 1.2 Å). However, the high redundancy of the data, the low goodness-of-fit value obtained, and the error estimates given above all indicate that the structure is well determined and suitable for drawing detailed inferences about the geometry of the vancomycin:acetate complex.

Results and Discussion

General Features of the Asymmetric Unit. Vancomycin is an asymmetric homodimer of the general type previously described for various glycopeptide antibiotics on the basis of NMR data,^{13,38–42} and as seen in the balhimycin structure of

Table 2. Hydrogen Bonding in the Dimer Interface

donor	acceptor	O...H Distance (Å)	C=O...H angle (deg)
V2:6	V1:3	2.29	170
V1:5	V2:5	2.14	149
V2:5	V1:5	2.03	163
V1:6	V2:3	2.22	164

Sheldrick et al.⁸ The two polypeptide chains are aligned antiparallel, and are related by an approximate 2-fold noncrystallographic symmetry axis (Figure 3). Hydrogen bonds connect the carbonyl groups of residues 3 and 5 on each monomer with the peptide hydrogens of residues 5 and 6 of the other monomer. The side chain aromatic rings of V1:4 and V2:6 are involved in edge-to-face interactions across the dimer interface, and there is a similar interaction between V1:6 and V2:4 (not illustrated). The aromatic rings of V1:5 and V2:5 also appear to interact, but through an edge-to-edge interaction in which their van der Waals surfaces are separated by 0.4 Å.

The interaction interface between disaccharide groups is extensive, and almost exclusively nonpolar. V1:G and V2:V both lie across the plane formed by the dimer interface, whereas V1:V and V2:G each form a portion of the concave recognition surface of their respective monomers (Figure 4). Overall, the asymmetry of the dimer is most pronounced in the disaccharide groups, but all of the monomer–monomer interactions deviate from 2-fold symmetry to some degree (Table 2).

Rigidity of the Macrocyclic Rings. V1 may be rotated and superimposed onto V2 with a root-mean-square difference of 0.18 Å for the 50 atoms comprising the three macrocyclic rings of residues 2–3–4, 4–5–6, and 5–6–7. Aligned in this manner, angles between corresponding aromatic ring planes vary from 2.1° for residue 4 to 7.7° for residue 7. The conformation of residue 1 is similar in both monomers, but χ_1 and χ_2 values for the side chain of residue 3 are different. The most conspicuous difference between the monomers, the orientation of the disaccharide groups, is largely the result of a 185° rotation about the phenolic ester bond connecting the disaccharide group to residue 4 (Figure 4).

The 50-atom macrocyclic rings of V1 and V2 superimpose nearly as well onto the corresponding atoms in balhimycin as they do onto each other (root-mean-square differences range from 0.15–0.35 Å), evidencing considerable structural rigidity in the core of both molecules. The vancomycin structures differ from balhimycin most notably in the nature and location of their sugar residues. In addition, the balhimycin dimer exhibits a pattern of side chain conformational differences between monomers that contrasts with that found in vancomycin: in vancomycin, the two monomers differ primarily at residue 3, whereas in balhimycin, the differences are relatively minor, and involve residues 1 and 7.

The spatial relationships between monomers in the balhimycin dimer are conspicuously different than those between monomers in the vancomycin dimer, despite identical hydrogen-bonding patterns. These differences may be due to differences between the sugar residues in each compound, different crystal packing forces, or the presence of the acetate ligand in V2. In any case,

(38) Waltho, J. P.; Williams, D. H. *J. Am. Chem. Soc.* **1989**, *111*, 2475–2480.

(39) Gerhard, U.; Mackay, J. P.; Mapleston, R. A.; Williams, D. H. *J. Am. Chem. Soc.* **1993**, *115*, 232–237.

(40) Groves, P.; Searle, M. S.; Mackay, J. P.; Williams, D. H. *Structure* **1994**, *2*, 747–754.

(41) Mackay, J. P.; Gerhard, U.; Beauregard, D. A.; Mapleston, R. A.; Williams, D. H. *J. Am. Chem. Soc.* **1994**, *116*, 4573–4580.

(42) Mackay, J. P.; Gerhard, U.; Beauregard, D. A.; Westwell, M. S.; Searle, M. S.; Williams, D. H. *J. Am. Chem. Soc.* **1994**, *116*, 4581–4590.

(33) Rollett, J. S. In *Crystallographic Computing*; Ahmed, F. R., Hall, S. R., Huber, C. P., Eds.; Munksgaard: Copenhagen, 1970; pp 167–181.

(34) Taylor, R.; Kennard, O. *Acta Crystallogr.* **1986**, *B42*, 112–120.

(35) Hamilton, W. C.; Abrahams, S. C. *Acta Crystallogr.* **1970**, *A26*, 18–24.

(36) Luzzati, V. *Acta Crystallogr.* **1952**, *5*, 802–810.

(37) Allen, F. H.; Kennard, O.; Watson, D. G.; Brammer, L.; Orpen, A. G.; Taylor, R. *J. Chem. Soc., Perkin Trans. 2* **1987**, *1987*, S1–S19.

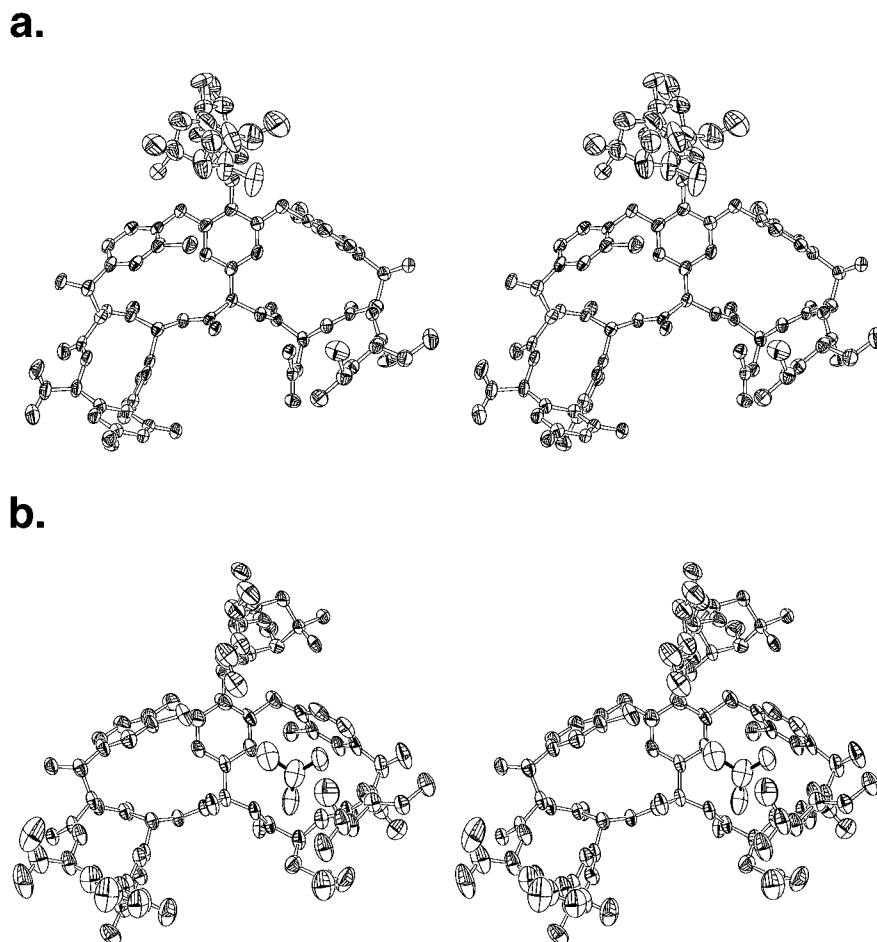


Figure 2. Stereoview of the anisotropic thermal ellipsoids for the two vancomycin monomers in the crystal asymmetric unit. Panel a shows molecule 1, while panel b shows molecule 2. Ellipsoids are drawn at the 50% probability level; in cases where conformational disorder has been identified, only the principal conformers are shown for clarity. The acetate ligand bound to molecule 2 is shown with dark bonds and no cross-hatching in the ellipsoids. The relatively large size of the ellipsoids for the carbohydrate residues illustrates that the sugars are considerably less rigid than the heptapeptide core. This appears to be due to the relative tightness of packing in the dimer interface. The two heptapeptides in the dimer are in close apposition, with several hydrogen bonds “cementing” the two monomers into position. In contrast, the carbohydrate halves of the dimer are only loosely packed; they are roughly complementary in shape, but not exactly, so only a few loose van der Waals interactions are made, and no strong hydrogen bonds connect the two disaccharides (see Figure 4). This loose packing allows the carbohydrates to be considerably more mobile than the heptapeptide core. Figure 2 was generated with the program ZORTEP.

these differences imply that interactions which stabilize dimers in this class of molecules are flexible. Therefore, while the gross features of these dimers may be common to many glycopeptide antibiotics, the specific interactions seen in balhimycin or vancomycin may not be general.

The V1 Recognition Surface. The surface regions of V1 believed to be involved in recognizing target ligands in the bacterial cell wall are largely occupied by residues 1 and 3 from a symmetry-related copy of V1. Cl-2 and a symmetry-related copy of V2 also associate with the C-terminal end of V1. These interactions completely exclude solvent water from the recognition surface of V1. For this reason, the polar moieties of V1 involved in ligand recognition must have alternative partners in this crystal structure. Accordingly, we find that the amide proton of V1:7 is hydrogen bonded to Cl-2, and that Cl-4 lies in close proximity to V1:1, compensating for its positive charge and serving as a hydrogen bond acceptor for the amide proton of V1:2. Of particular note, the amide protons of V1:3 and V1:4 and the carbonyl oxygen of a symmetry-related copy of V1:4 all form intramolecular hydrogen bonds with the side chain of V1:3. The significance of this configuration is discussed further below.

The V2:Acetate Complex. The surface of V2 involved in ligand recognition faces a large solvent channel in the crystal

and is occupied by a single acetate molecule, a chloride ion, and water (Figure 5). One of the acetate oxygens forms a hydrogen bond with V2:2 ($r_{O\cdots H} = 1.97 \text{ \AA}$, $\theta_{C=O\cdots H} = 165^\circ$), while the other is involved in a bifurcated hydrogen bond with V2:3 ($r_{O\cdots H} = 2.08 \text{ \AA}$, $\theta_{C=O\cdots H} = 154^\circ$) and V2:4 ($r_{O\cdots H} = 2.07 \text{ \AA}$, $\theta_{C=O\cdots H} = 111^\circ$). The acetate does not interact directly with the charged *N*-methyl terminus of V2:1, but makes van der Waals contact with several parts of its hydrophobic side chain. The methyl group of the acetate simultaneously interacts with the ring face of V2:4, the chlorine atom of V2:6, and a hydroxyl group of V2:G. The amide protons of V2:4 and V2:7 form hydrogen bonds with a solvent water and Cl-3, respectively.

It is remarkable and significant that there are no interactions between the Asn side chain of V2:3 and the acetate ligand (Figures 2 and 5), particularly in light of altogether different conclusions reached in a recent NMR and computational study of a compound identical to vancomycin except for a monosaccharide on residue 6 (A82846B).¹³ That work concluded that one carboxylate oxygen forms a bifurcated hydrogen bond to residues 2 and 3, while the other forms a bifurcated hydrogen bond to the Asn side chain of residue 3 and the main chain amide proton of residue 4. One should note, however, that the hydrogen bond relationships in A82846B were not defined by

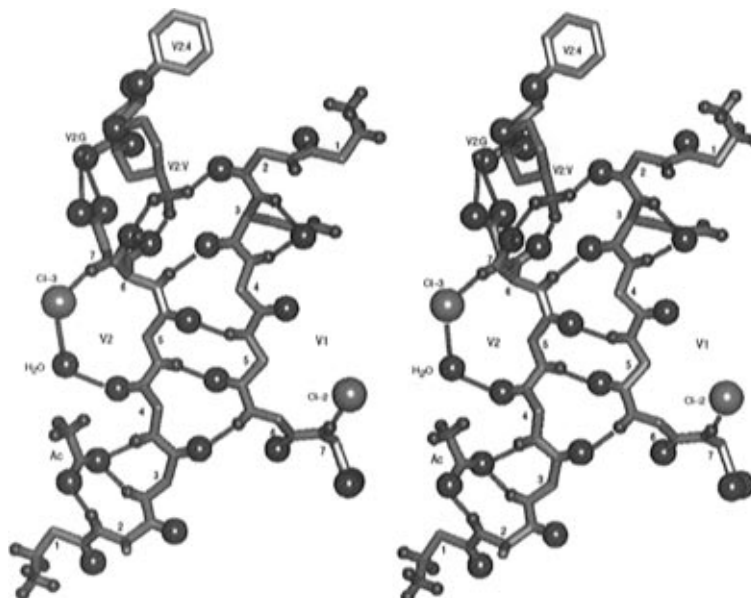


Figure 3. Stereoview of the antiparallel relationship between heptapeptide backbones, showing the hydrogen bond pattern between V1 (right) and V2 (left), as well as between V2 and the acetate ligand (Ac). Note that the Asn side chain of V1:3 forms hydrogen bonds with amide protons of V1:2 and V1:3. Carbohydrate moieties from a symmetry-related molecule in the crystal lattice are shown at the top left of the figure; both V2:G and V2:V from this symmetry-related molecule are seen to form specific polar interactions with both V1 and V2. Two of the chloride ions found in the crystal lattice are shown in this figure, as well as a water molecule found next to the acetate molecule in the V2 ligand binding site. Chloride ions, oxygen atoms, and hydrogen atoms are shown as large, medium, and small spheres, respectively.

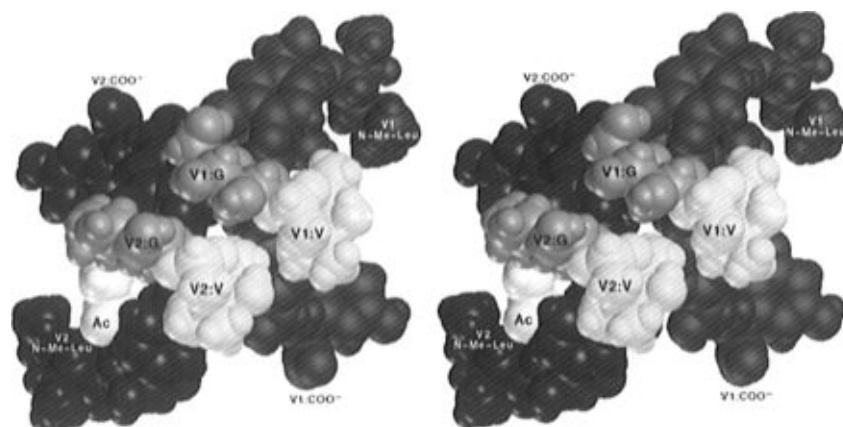


Figure 4. Stereoview of the vancomycin dimer:acetate complex, showing a space-filling model viewed along the local symmetry dyad. Spheres correspond to van der Waals radii. The N- and C-termini of the peptide chains are labeled. Note that V1:G and V2:V lie across the dimer interface, and that the acetate (Ac) bound to V2 interacts only with V2:G.

the NMR data, but were inferred from computer simulations. Thus, our crystallographic data do not necessarily contradict the original NMR data of Prowse et al., but they do point to a substantially different conclusion.

The crystal structure reveals an intriguing role for the Asn side chain, namely that of a surrogate hydrogen bond partner for the amide protons of V1:3 and V1:4 in the absence of ligand (illustrated in Figures 2, 3, and 5). This role appears to be important, insofar as structure–activity relationship studies clearly implicate this side chain as essential for antimicrobial activity.² Sheldrick et al.⁸ suggested that the Asn side chain may function as a “flap” which moves to allow ligand to enter and leave the binding pocket. However, this does not explain why this side chain is essential for activity. The V2:3 Asn side chain does not participate in the recognition of the acetate ligand bound to V2. However, the V1:3 Asn side chain partially occupies the V1 ligand binding site. Therefore, we speculate that this may promote ligand binding activity by preventing solvation or facilitating desolvation of the binding site. If the Asn side chain was not present, a water molecule occupying

the concave and highly polarized binding pocket in place of a ligand might be difficult to displace.

The protonation state of the acetate molecule is not obvious from this structure; the crystallization conditions (pH = 4.6) allow for either a protonated or an unprotonated species. No hydrogen atom is seen in the Fourier difference map, but this is not conclusive because not all hydrogen atom density is expected to be visible above the noise of the map. A comparison of the carbon–oxygen bond lengths is more instructive: The two carbon–oxygen bonds in the acetate molecule have lengths of 1.305 ± 0.014 and 1.279 ± 0.016 Å. These values are within two standard deviations of the ideal value for carbon–oxygen bond lengths in RCOO^- ; however, they are substantially longer than the expected value of 1.214 ± 0.019 Å for the carbonyl bond in a protonated carboxylic acid.³⁷ This result, as well as the observation of Prowse et al.⁴³ that the pKa of the ligand carboxylate bound to a closely related antibiotic was “deeply depressed”, weigh in favor of the anionic form of

(43) Kline, A. Personal communication.

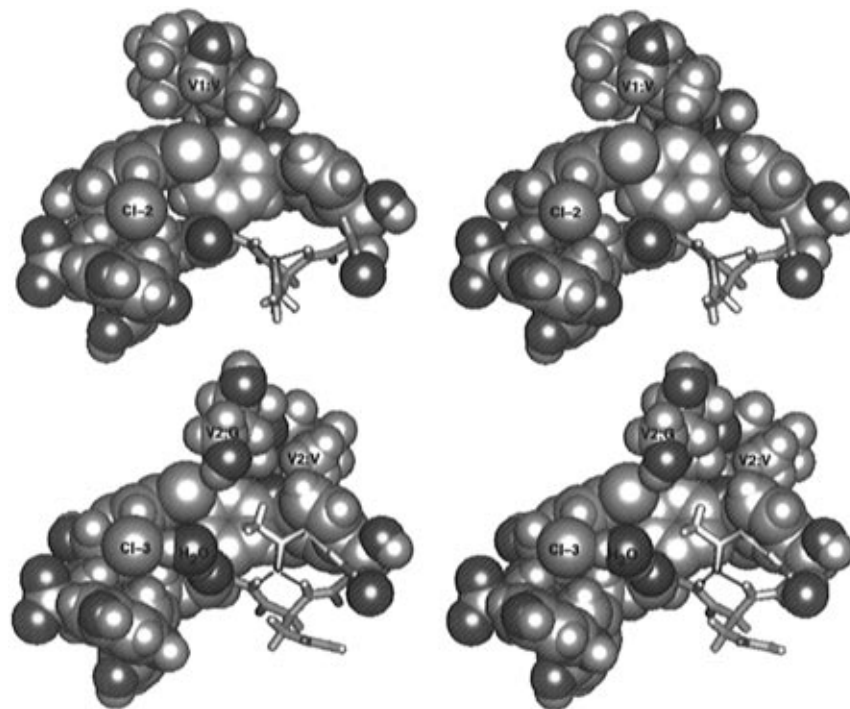


Figure 5. Stereoviews of the ligand pockets of V1 and V2. The upper panel shows V1 and the lower shows V2. The molecules are drawn as space-filling spheres at 70% van der Waals radii, except for residues 2, 3, and 4 and the acetate, which are shown as stick models. The side chains of V1:1 and V2:1 have been deleted for clarity; these side chains, if included, would largely obscure the binding pockets from this perspective. Oxygen atoms are shown as dark spheres. Upper panel: Hydrogen bonds are shown between the oxygen atom of the V1:3 side chain and the amide protons of V1:3 and V1:4 (dashed lines). A chloride ion is seen at the left of the binding pocket; this ion interacts with the amide group of V1:7 and with the edges of the aromatic rings of V1:5 and V1:6. Note that, in addition to the V1:3 side chain and this chloride ion, the V1 binding pocket is occupied by atoms contributed by a symmetry-related V1 molecule (not shown). Lower panel: Hydrogen bonds between the acetate and the amide protons of V2:2, V2:3, and V2:4 are shown as dashed lines. V2:G (top, center) overhangs the binding site. Note that the acetate methyl group interacts simultaneously with V2:G, the aromatic ring edge of V2:2, the aromatic ring face of V2:4, and the chlorine of V2:6. Note also that the side chain of residue 3 does not interact with the ligand. A chloride ion is also found to the left of the V2 binding pocket, in an environment similar to that of the chloride ion bound to V1.

the ligand. This depression of the carboxylate pK_a is reasonable on theoretical grounds, since the convergence of backbone peptide dipoles from residues 1–4 likely creates a highly positive electrostatic potential in this region.

Implications for Natural Ligand Binding. Acetate is known to bind specifically to vancomycin, although its affinity is lower than those of di- and tri-peptides containing the D-Ala-D-Ala sequence.⁴⁴ Thus, the details of acetate binding revealed by this structure should be relevant to general questions of ligand recognition by vancomycin. This crystal structure reveals a well-defined single orientation for the acetate ligand, but it provides no clear reason why it preferentially binds to V2. This preference may simply reflect crystal lattice effects, and be unrelated to affinity preferences in solution.

The interaction between the ligand's carboxylate group and the drug is of central interest. While many of the features seen in this crystal structure were anticipated by earlier NMR studies of vancomycin and related compounds, they left the precise nature of carboxylate recognition somewhat ambiguous. For example, Prowse et al.¹³ suggest that the carboxylate group may assume more than one orientation in the binding pocket of A82846B, and that the side chain of residue 3 is an integral part of the hydrogen-bonding network. On the other hand, multiple binding modes are not suggested in studies of eremomycin–ligand complexes, nor is a role for Asn 3.^{40,45} The NMR and molecular mechanics study of dipeptide binding to the vancomycin aglycon by Li et al.¹⁹ concurs with the latter. While

the differences between the various NMR studies may be due to the use of different ligands and different antibiotics, one must be cautious with inferences at this level of detail drawn from NMR studies to the extent that they depend on conditioning and final refinement by molecular mechanics, and thus are subject to the pitfalls inherent in these procedures and parameter sets.

It remains unclear how dimerization enhances the binding of ligands by vancomycin. MacKay et al.⁴² suggested that hydrogen bonds across the dimer interface may reduce dynamic fluctuations of the heptapeptide backbone and thereby stabilize hydrogen bonds between the backbone and the ligand. The crystallographic data appear to weigh against this explanation because the shape of the macrocyclic rings in vancomycin and balhimycin is tightly conserved in spite of differing hydrogen bond geometries. We interpret this as evidence that structural rigidity is an inherent property of these molecules, irrespective of whether their backbones are hydrogen bonded.

In lieu of a plausible quasimechanical explanation for enhanced ligand affinity in the dimer, we suggest that one or more peptide groups involved in hydrogen bonds to a ligand are electronically polarized by virtue of being also involved in hydrogen bonds across the dimer interface (Figure 3). In the case of the vancomycin dimer, this effect would be limited to the peptide groups on either side of residue 4. MacKay et al.⁴² have suggested that in compounds with charged monosaccharides on residue 6, a similar polarization effect may involve the critical peptide group joining residues 2 and 3. This would account for the small but real effect of dimerization on ligand

(44) Pierce, C. M.; Gerhard, U.; Williams, D. H. *J. Chem. Soc. Perkin Trans.* **1995**, 2, 159–162.

(45) Williams, D. H. *Acc. Chem. Res.* **1984**, 17, 364–369.

affinity seen in vancomycin, and the significantly greater effect seen in compounds such as ristocetin, eremomycin, and A82846B.

Acknowledgment. The authors gratefully acknowledge data collection advice and assistance from Lisa Keefe, Stephan Ginell, and Randy Alkire of the Argonne National Laboratory Structural Biology Center, useful advice and discussions about the use of SnB contributed by Russ Miller, and comments on the manuscript from Dudley Williams. The Argonne National Laboratory Structural Biology Center at beamline X8C of the National Synchrotron Light Source is supported by USDOE Office of Health and Environmental Research. P.J.L. was

supported by grants from the McCabe Foundation and the Research Foundation of the University of Pennsylvania and an Institutional Research Grant from the American Cancer Society; P.H.A. was supported by GM50805, a grant-in-aid from the SE Pennsylvania Affiliate of the American Heart Association, and a Biomedical Scholar Award from the L. P. Markey Charitable Trust.

Supporting Information Available: Color versions of Figures 3–5 are available. See any current masthead page for ordering and Internet access instructions.

JA963566P